

Assessment of heating effects in skin during continuous wave near infrared spectroscopy

Y. Ito

Hitachi Central Research Laboratory
Kokubunji-shi, Tokyo, Japan 815-8601

R. P. Kennan

Hitachi Central Research Laboratory
Kokubunji-shi, Tokyo, Japan;
Yale University School of Medicine
Department of Diagnostic Radiology
New Haven, Connecticut 06511

E. Watanabe

Tokyo Metropolitan Police Hospital
Department of Neurosurgery
Chiyoda-ku, Tokyo, Japan 102-8161

H. Koizumi

University of Tokyo
Graduate School of Arts and Sciences
Meguro-ku, Tokyo, Japan;
Hitachi Advanced Research Laboratory
Hatoyama-shi, Saitama, Japan 350-0395

Abstract. Near infrared spectroscopy is an increasingly important tool for the investigation of human brain function, however, to date there have been few systematic evaluations of accompanying thermal effects due to absorption. We have measured the spatial distribution of temperature changes during near infrared irradiation (789 nm) as a function of laser power, in both excised tissue (chicken meat and skin) and in the forearm of an awake human volunteer. Light was applied using a 1 mm optical fiber which is characteristic of the topographic system. The temperature of excised chicken tissue increased linearly with power level as 0.097 and 0.042°C/mW at depths of 0 and 1 mm, respectively. Human forearm studies yielded temperature changes of 0.101, 0.038, and 0.030°C/mW at depths of 0.5, 1.0, and 1.5 mm, respectively. Due to direct irradiation of the thermocouple all measurements represent the maximum temperature increase from the laser. In all cases the estimated heating effects from continuous wave optical topography systems were small and well below levels which would endanger tissue cells. The close similarity between *ex vivo* and *in vivo* measurements suggests negligible contributions from blood flow in the skin which was further supported by measurements during cuff ischemia. Heating effects decreased sharply with both depth and lateral position; thus, for optode spacings greater than a few millimeters, fibers can be treated independently. Finite element analysis confirms that the experimental results are consistent with a simple heat conduction model. © 2000 Society of Photo-Optical Instrumentation Engineers. [S1083-3668(00)00104-0]

Keywords: optical imaging; near-infrared spectroscopy; laser heating.

Paper JBO-90032 received June 2, 1999; revised manuscript received Apr. 4, 2000 and June 2, 2000; accepted for publication June 7, 2000.

1 Introduction

It has long been known that light is sensitive to chromophore concentration in living tissue.^{1,2} Due to the relative transparency of tissue in the near infrared region, optical methods can now be used as an effective *in vivo* probe.^{3,4} Near infrared spectroscopy allows the noninvasive differentiation between tissues which possess different absorption or scatter and provides spectroscopic information on chromophore concentrations such as hemoglobin and cytochrome. In the field of brain research, these methods have been successfully employed to monitor global brain oxygenation changes, during hypoxia,⁵ and local hemoglobin oxygenation changes associated with neural activity.^{6–9} Optical topography was proposed as a new method for visualizing brain activity by using multiple optodes simultaneously¹⁰ to obtain a spatial map of absorption changes using reflected light from the cortical surface. Devices developed have been used to monitor spatio-temporal blood volume and oxygenation in cortices during sensory stimulation,^{10,11} cognitive function,¹² and epileptic seizures¹³ and facility of the device can allow noninvasive measurement of human brain function under a variety of conditions without subject restriction. Optical topography sys-

tems developed in this lab currently use wavelengths near the 799 nm isobestic point for oxyhemoglobin and deoxyhemoglobin which are convenient for the simultaneous determination of oxy-, deoxy-, and total hemoglobin changes. Light is guided to the skin surface via an array of optical fibers.¹⁰ A source of concern in the application of near infrared systems is the heating effects, which will occur maximally near the skin surface beneath the optical fiber. While current continuous wave topography systems operate at power levels consistent with a class 2 laser it is nonetheless important to determine the heating effects incurred in biological systems so as to insure that tissue is not put in harm's way. This is especially important in applications involving human neonates where transcranial near infrared methods have been shown to be particularly effective due to the thin skull and relative optical transparency compared to adults.⁵ Mechanisms responsible for tissue damage are a complex function of heat exposure, which are still poorly understood. Previous studies have shown that when cell temperatures are sustained above 41°C there is an increased likelihood of cell death.^{14,15} While the effects of ultraviolet irradiation on tissue is well documented¹⁶ there have been few studies on the effects of low level near infrared radiation on living systems. Reports involving laser

Address all correspondence to H. Koizumi. Tel: 81-0492-96-6111 Ext. 200; Fax: 81-0492-96-6606; E-mail: hkoizumi@harl.hitachi.co.jp

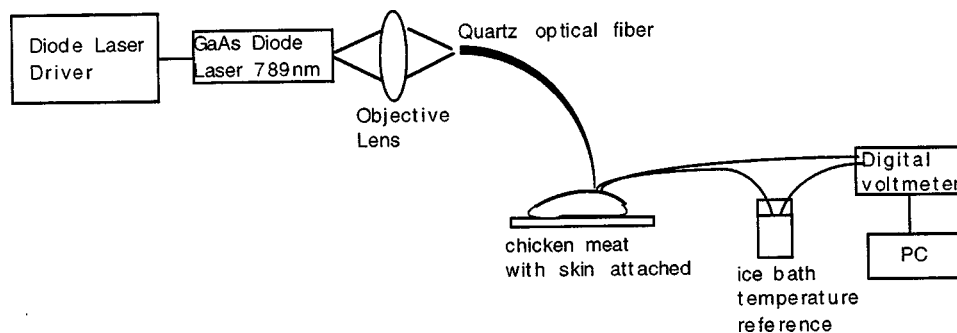


Fig. 1 Experimental setup for temperature measurement during near infrared illumination.

surgery techniques have shown that infrared irradiation can lead to slight latencies in median nerve conduction and concomitant small decreases in local skin temperature.¹⁷ In order to evaluate the thermal heating effects from near infrared irradiation in optical topography we have performed experiments using excised tissue (chicken meat with attached skin). For living mammals, the ability of the skin to dissipate heat is crucial to normal physiologic function. It is well known that local heating of skin can lead to activation of thermal receptors, which induces local vasodilatation. This blood flow increase can serve to regulate temperature in that area. At higher temperatures other cooling mechanisms are brought into play such as sweating.¹⁸ Hence, it is likely that heating effects will be somewhat different in living tissue and excised tissue samples. To test this hypothesis a parallel set of experiments were also performed on the forearm of an awake human subject to evaluate the temperature rise just below the skin surface. The results are then compared to computer simulations using a simple heat conduction model.

2 Methods

Figure 1 illustrates the experimental setup for the measurement. A GaAs laser diode was employed at a wavelength of 789 nm, which is in a range appropriate for most *in vivo* studies. The power of the laser diode was controlled by a variable driving current. Light was directed via a 1 mm aperture quartz optical fiber, which was placed on the surface of the skin. Fibers of this size are currently employed in our transcranial system to minimize light scattering effects from hair and insure good optical contact with the scalp.¹⁰ Temperature was monitored with a C.A. thermocouple (Wells Industrial Thermometers) with a diameter of 0.25 mm. The sensing element of the thermocouple was painted white to minimize direct absorption effects. Data were acquired continuously and stored on a PC. The laser was cycled on for five cycles of 40 s illumination followed by 40 s of recovery. Slow base line drifts in ambient temperature in the absence of laser illumination were linearly corrected. Temperature changes were determined by averaging the steady state temperatures, in which we allowed at least 20 s for nonsteady state heating and cooling. Laser power levels ranged from 1 to 9.8 mW which corresponds to irradiance, I , at the fiber tip of $I = 127$ to $I = 1273$ mW/cm². Since the fiber diameter is constant in all experiments, we refer to variations in the laser power level to describe the irradiation. As a useful comparative guide, optical topography is typically employed in a range of 0.5–1 mW

that corresponds to 68 mW/cm² $< I < 127$ mW/cm². The irradiance due to sunlight on the earth's surface is approximately 100 mW/cm² and is more efficiently absorbed than near infrared light.¹⁹

Ex vivo experiments were performed using a sample of chicken meat with intact skin. Temperature changes were measured on the skin surface and at a depth of 1 mm. The thermocouple tip was placed at a depth of 1 mm below the surface of the skin using an injector needle as illustrated in Figure 2. By fixing the angle of injection we could easily monitor the depth of the needle by recording the length injected. The thermocouple was injected 1.7 mm from the center of the fiber at an angle of approximately 30° such that it was directly below the incident light source at a depth of 1 mm. Temperature changes were recorded as a function of thermocouple depth, and laser power. Since excised tissue has no capacity to thermoregulate, we assume that this model will yield an upper limit estimate of the temperature rise expected in tissues.

In vivo experiments were also performed on the forearm of a human subject. The thermocouple was carefully inserted via a hypodermic needle to depths of 0.5, 1, and 1.5 mm below the skin surface of the forearm using the same technique as described above. The radial extent of heating was measured by moving the beam axis away from the thermocouple at a fixed depth of 0.5 mm. To determine whether blood circulation plays a role in thermoregulation at these low power levels, we repeated the irradiation measurements at 9.8 mW during cuff ischemia with a prolonged 5 min exposure.

To estimate the role of conductive cooling we also performed a finite element simulation of heating effects in a model system with the thermal properties of bulk water. A $20 \times 20 \times 20$ rectangular grid of 0.5 mm elements was used to model a 1 cm³ volume that is assumed to initially be at uniform temperature. The time evolution of the temperature element, T_{ijk} , at time, $t + \delta t$, is given by²⁰

$$T_{ijk}(t + \delta t) = T_{ijk}(t) + \frac{1}{C} \left(\left\{ \sum_{nn} K [T_{ijk}(t) - T_{nn}(t)] \right\} + dq_{ijk} \right) \delta t, \quad (1)$$

where the subscripts ijk denote the element of interest and the summation over nearest neighbors is given by nn . Heat flow into the system is determined by dq_{ijk} and is assumed to be

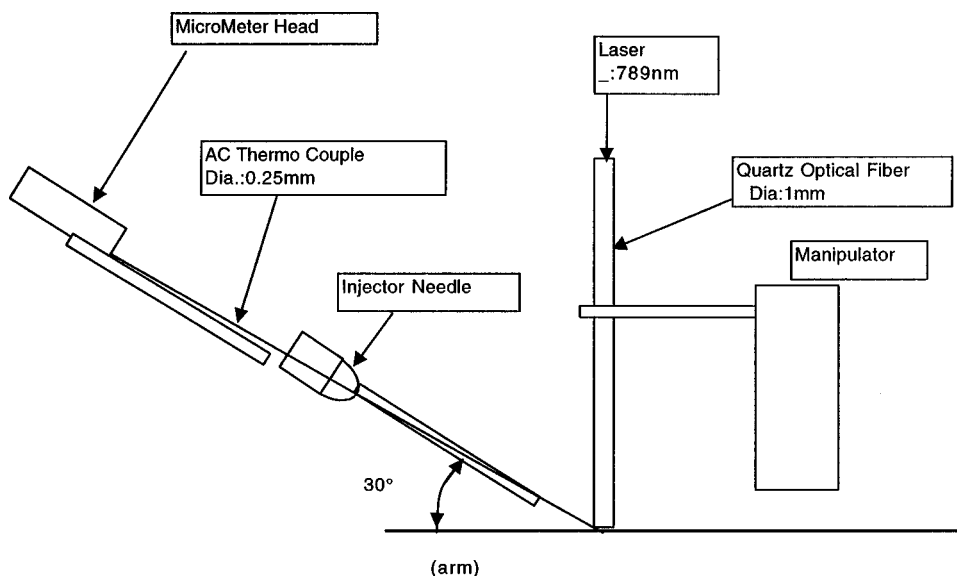


Fig. 2 Depiction of the thermocouple insertion beneath the optical fiber.

uniformly absorbed within 1 mm of the surface. Heat was added to a central region of 3×3 elements (0.0225 cm^2) at a rate of $dq = 120\text{--}1200 \text{ mW/cm}^2$. Heat flow from element, ijk , to neighboring elements, nm , is determined by the coefficient $K = kA/L$, where k is the thermal conductivity, L is the element length (0.5 mm), and A is the surface area through which heat flows ($A = L^2$ for this geometry). C denotes the heat capacity of each element which is given by $c\rho V$, where c is the specific heat ($\text{J/g}^\circ\text{C}$), ρ is the density (g/cm^3) and V is the volume of the element ($V = AL$). The temperature at the boundaries far from the source was held constant and surface convection was neglected. Time steps, δt , were chosen such that $\delta t < C/6 \text{ K}$, which insures system stability.²⁰ Values of $k = 600 \text{ mW/m}$, $c = 4.2 \text{ J/g}^\circ\text{C}$, and $\rho = 1 \text{ g/cm}^3$ were assumed for bulk water.²¹

3 Results

3.1 Power Dependence and Depth Dependence in Excised Tissue

Figure 3 shows the change in temperature during infrared irradiation at a power level of 9.8 mW. Typically, the tempera-

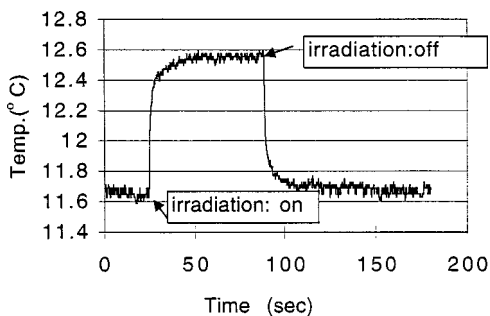


Fig. 3 Temperature recording during laser 789 nm continuous illumination as a function of time in excised tissue sample. The power level of the laser diode was 9 mW.

ture reached equilibrium by 10–20 s, after which thermal losses to the surrounding environment balanced the absorbed energy. The mean temperature change at the skin surface, ΔT , was then measured as a function of laser power level. Each temperature measurement shown was averaged five times at a given power level, which was varied from 1 to 9.8 mW ($I = 127\text{--}1273 \text{ mW/cm}^2$). These results are illustrated in Figure 4. Regression yields a linear slope that is approximately 0.1°C/mW . The thermocouple was then positioned to a depth of approximately 1 mm and temperature changes were measured at power levels of 5 and 9 mW. Figure 5 shows the measured temperature changes at this depth. The estimated dependence of the temperature rise on power level is found to be 0.042°C/mW . These results are summarized in Table 1.

3.2 In vivo Results

3.2.1 Power and depth dependence

Figure 6 shows the temperature rise as a function of laser power at depths of 0.5, 1, and 1.5 mm directly below the fiber. Each temperature measurement was repeated five times at a

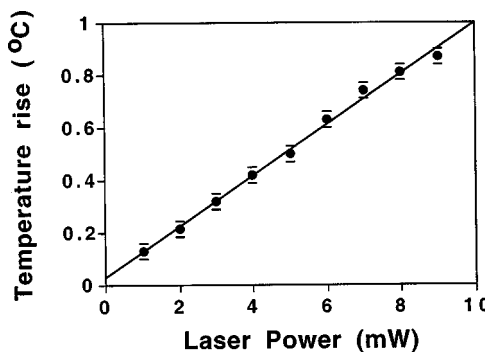


Fig. 4 Temperature rise as a function of power level on the skin surface on the excised chicken tissue. The slope of the fitting curve is 0.0965°C/mW .

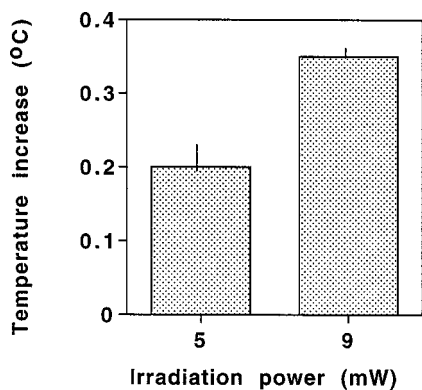


Fig. 5 Change in temperature at a depth of 1 mm in excised chicken tissue. Data are shown for 5 and 9 mW illumination.

given power level, which was varied from 2 to 9.8 mW ($I = 254\text{--}1273\text{ mW/cm}^2$). For 40 s exposures the total energy absorbed ranged from 0.04 to 0.39 J. The temperature rise once again demonstrates a clear linear dependence with laser power level where the slope decreases sharply between 0.5 and 1 mm. The data are summarized in Table 1. It is apparent that at power levels characteristic of optical topography (1 mW) the tissue rapidly dissipates heat as a function of tissue depth thus insuring that deeper tissue will not be adversely affected.

For *in vivo* studies we sometimes observed blood on the tip of the thermocouple, which leads to slightly larger temperature rises during infrared irradiation. In these circumstances the effects of blood on the sensor could be accounted for by repeating the temperature measurement at a fixed power level of 9.8 mW in a subcutaneous region which did not show any bleeding, thus determining the fractional change due to direct heating. We attribute this to direct absorption of dried blood on the thermocouple tip. By repeating the measurement with a clean tip we could obtain a fairer estimate of the changes within tissue itself. We note that there may still be a residual contribution to the temperature rise due to absorption on the thermocouple itself, so the results obtained in these experiments should be considered maximal estimates of infrared heating of the tissue. In order to roughly estimate the effects of direct irradiation on the thermocouple, we measured the temperature changes at a depth of 1 mm in chicken skin with

Table 1 Summary of depth dependence data.

System	Depth (mm)	Maximal temp. rise per mW through 1-mm-diameter fiber (°C/mW)	Maximal temp. rise per unit irradiance (°C/mW/cm ²)
Chicken skin	0 mm	0.0965 ± 0.001	7.58 × 10 ⁻⁴
	1 mm	0.042 ± 0.004	3.30 × 10 ⁻⁴
Human forearm	0.5 mm	0.101 ± 0.001	7.93 × 10 ⁻⁴
	1 mm	0.038 ± 0.001	2.95 × 10 ⁻⁴
	1.5 mm	0.029 ± 0.0005	2.28 × 10 ⁻⁴

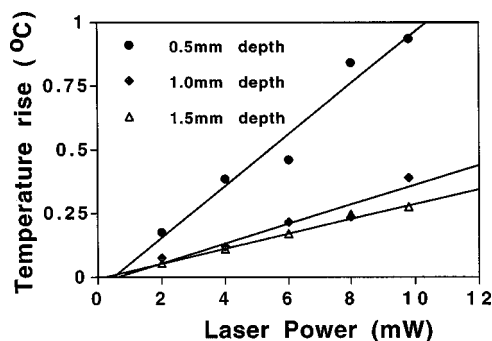


Fig. 6 Temperature rise as a function of power level and depth from human forearm. The slope of the fitting curves is summarized in Table 1.

the thermocouple painted black and then painted white. The estimated spectral reflectivities in each were 0.03 and 0.7, respectively.²¹ The corresponding temperature rises measured were 0.099°C/mW for the black thermocouple and 0.039°C/mW for the white thermocouple. Assuming a linear relationship between reflectivity and temperature we estimate that in the limit of perfect reflectivity the temperature rise should be 0.012°C/mW. This means that the measured values for temperature rise in human forearm and chicken meat are probably overestimated by a factor of ~3 though we prefer to remain cautious and present the data as the maximum temperature rise.

3.2.2 Spatial distribution of temperature changes

Figure 7 shows the temperature increase as a function of radial distance from the beam axis during 9.8 mW illumination at a depth of 0.5 mm. It is apparent that the heating effects are localized to within a few millimeters of the beam axis. These data can be combined with the depth dependence data along the beam axis to map the temperature rise during 9.8 mW illumination. Two-dimensional Gaussian interpolation yields the spatial temperature rise map shown in Figure 8.

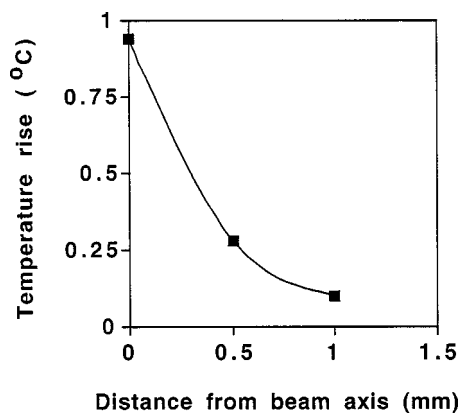


Fig. 7 Temperature rise during 9.8 mW irradiation at 0.5 mm depth as a function of radial distance from the beam axis (mm) in human forearm.

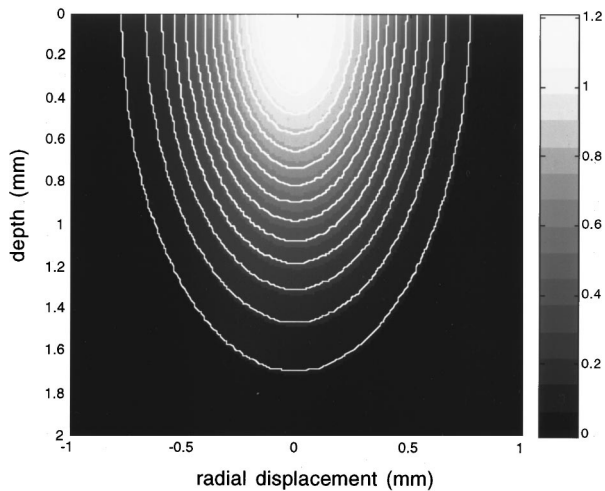


Fig. 8 Interpolated temperature map for 9.8 mW irradiation in human forearm with overlaid contour map. Temperature change for outermost contour is approximately 0.2°C .

The maximum temperature rise is $\sim 1.2^{\circ}\text{C}$ at the surface while the outermost contour designates a temperature rise of approximately $\sim 0.2^{\circ}\text{C}$.

We expect that the spatial dependence of the temperature measurements should be similar to the photon fluence rate. At wavelengths near 800 nm the absorption (μ_a) and scattering (μ_s') coefficients for skin range from $0.02\text{--}0.3\text{ mm}^{-1}$ and $2.1\text{--}2.4\text{ mm}^{-1}$, respectively.²² For the case of continuous radiation this yields a range of optical penetration depths,²³ $1/\mu_{\text{eff}} = 1/[3\mu_a(\mu_a + (\mu_s')^{1/2})]^{1/2}$, of $0.7\text{--}2.8\text{ mm}$. Although the optical properties of skin have previously been determined, it is difficult to use these values to estimate the fluence at small depths since analytic expressions derived from diffusion theory are invalid at small length scales (less than $1/\mu_s'$). As a rough estimate of the fluence rate through chicken skin we experimentally measured the collimated transmission coefficient through a 1-mm-thick sample. Light was detected through a 1 mm aperture on the surface of the sample. The fluence, ϕ , was estimated as the ratio light detected through the aperture with and without the skin, I/I_0 . For skin of 1 mm thickness $I/I_0 \cong 0.22$, while at 2 mm $I/I_0 \cong 0.05$.

Optical topography provides the simultaneous evaluation of oxygenation changes at multiple spatial positions and therefore employs a multi-optode acquisition scheme.¹⁰ Under these conditions it is important to evaluate the cumulative effects of light absorption from the multi-optode arrangement. Figure 8 shows that heating effects are clearly localized to within 1 or 2 mm of the illumination region. Therefore, when optodes are positioned more than a few millimeters apart there should be no long-range cumulative effects and each fiber can be treated independently. For transcranial topography on adults, optode spacings are typically 2–4 cm which allows the light to reach the cerebral cortex.^{3,10} For neonates the spacing should be reduced to 1 cm to accommodate the thinner skull. In both cases this spacing is sufficient to treat each fiber independently.

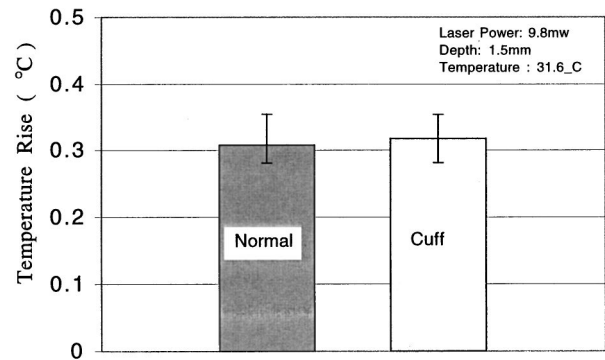


Fig. 9 Effects of cuff ischemia during 9.8 mW irradiation at depth of 0.5 mm.

3.2.3 Effects of circulation

Temperature regulation is a classic example of a biological control system. The balance between heat production and loss is continuously perturbed by changes in metabolic rate and external environment. Variations are detected by thermoreceptors in the skin that can initiate various compensatory reflexes.¹⁸ These systems are thought to be integrated in the hypothalamus but other brain centers may be involved as well. One important mechanism for thermoregulation is convection via the control of blood flow to the skin. By increasing blood flow the skin can effectively change its insulating properties with respect to the body core. For example, as blood flow is increased the core and skin temperatures become more closely associated. Thus when the external environment is very cold there is vasoconstriction in order to increase core insulation, whereas heat stimulation often stimulates vasodilation in order to increase heat loss. These effects become more complicated when the heating effect is localized to a small region. Similar thermoregulation effects may have important consequences in the brain function as well, and may partially account for the well-known increase in blood flow following increased metabolic activity, which appears to overcompensate for metabolic oxygen demand alone.

Figure 9 shows the temperature rise during 9.8 mW irradiation at a depth of 0.5 mm with and without cuff ischemia. It is apparent that there is little difference between these two cases. Furthermore, as shown in Table 1, we observed comparable temperature changes in the excised tissue system in which there is no blood flow. Thus, for optical topography, infrared light at power levels below 10 mW ($I < 1273\text{ mW/cm}^2$) do not evoke significant thermoregulatory response mechanisms and simple conductive cooling is adequate.

It has been shown that for ultraviolet illumination there is often a delayed temperature response in tissue which is correlated to the release of vasoactive substances¹⁶ which is characteristic of ultraviolet erythema. In order to insure that the temperature changes had reached a steady state, we performed an experiment with a 5 min illumination at 9.8 mW. The temperature reached a steady state after the first 30 s of exposure. Furthermore, after illumination was ceased the temperature returned to base line values within 30 s. This implies that the levels of irradiation employed were below those required

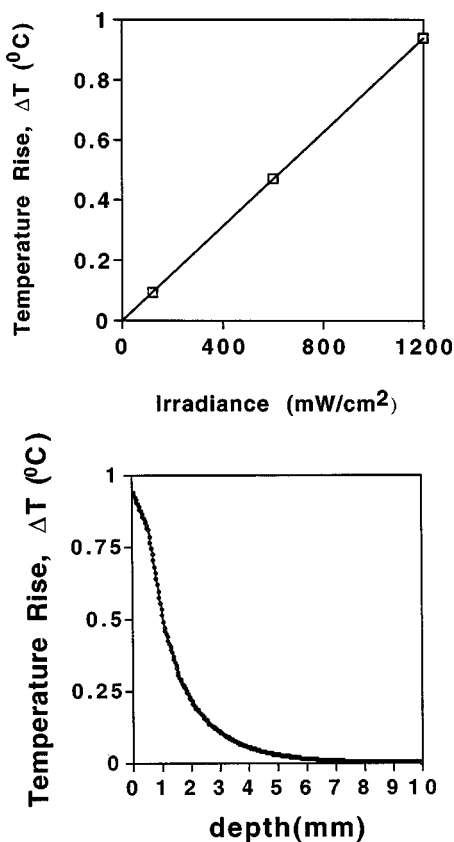


Fig. 10 (a) Maximum temperature rise for finite element analysis of 8 cm^3 aqueous system as a function of irradiance (mW/cm^2). Simulation details are given in the text. (b) Interpolated temperature rise as a function of depth during $1200 \text{ mW}/\text{cm}^2$ irradiation.

to elicit physiologic reactions. This will be discussed in more detail in the next section.

3.3 Simulation Results

Figure 10(a) shows the maximum temperature rise during continuous wave (CW) irradiation for finite element analysis of bulk water. Figure 10(b) shows the temperature rise as a function of depth during $1200 \text{ mW}/\text{cm}^2$ irradiation. For this model temperature regulation is achieved by conduction mechanisms alone. We can see over a comparable range of power deposition, temperature changes are maximally estimated to be $\Delta T(\text{max})=0.94^{\circ}\text{C}$, and at a depth of 0.5 mm the interpolated temperature rise is $\Delta T(0.5 \text{ mm})=0.81^{\circ}\text{C}$ which is within 20% of that obtained experimentally. This excellent agreement may be fortuitous, since this model is oversimplified, though it does support the argument that small temperature changes observed experimentally are consistent with efficient conduction of heat from the small region of irradiation. A more complete model could include convection from the tissue surface as well as temperature gradients from the skin to deeper tissue. The former would tend to increase the cooling efficiency by incorporating another cooling mechanism while the latter should decrease cooling efficiency since thermal conduction gradients from the irradiated tissue are reduced.

4 Discussion

The effects of heat on tissue has been studied extensively, however, due to the vast complexity of interactions, there is no single hypothesis for the long term effects of heat exposure.²⁴ Dewey et al. have demonstrated that prolonged exposure to heat above 41°C causes significant cell death,^{14,24} however, the maximum temperature which tissue will tolerate is closely related to the exposure time. The observation that cell death is not exclusively determined by the total energy deposited implies that the time-averaged kinetic energy is not the sole or even primary quantity that determines the life or death of the individual cell. Dewey has used empirical data to evaluate relationships between temperature and exposure time, which is consistent with thermodynamic arguments, based on reaction activation energies.²⁵ This information will be important in the evaluation of the effects of pulsed lasers since short duration pulses could generate brief yet very high temperature changes. While there is research in this direction^{26,27} it is beyond the scope of the current work. Low intensity continuous infrared laser light induced a maximal temperature change of approximately $0.1^{\circ}\text{C}/\text{mW}$ on the skin surface and $0.04^{\circ}\text{C}/\text{mW}$ at a depth of 1 mm in *ex vivo* tissue samples. For the forearm measurement we found very similar temperature changes which ranged from 0.11 to $0.02^{\circ}\text{C}/\text{mW}$ at depths of 0.5–1.5 mm, respectively. Skin surface temperature under normal conditions is usually near 31°C (Ref. 18) (depending on ambient conditions) thus a sustained change on the order of 10°C would be required for tissue damage. This is almost 100 times greater than the maximum rise during 1 mW CW irradiation.

4.1 Comparison with Previous Studies

While there has been a great deal of attention paid to the role of ultraviolet irradiation on tissue damage there is less literature on near infrared interactions. Recently there has been a new interest in the effects of near infrared laser light with regard to laser surgery procedures and low intensity laser therapy.^{17,28–30} In the later case the mechanisms of analgesia are still not well understood and remain controversial. We shall now summarize the results of these studies.

Basford et al.²⁸ have reported that irradiation with 830 nm CW laser light for 30 s over points on the forearm resulted in small but measurable motor and distal latencies in median nerve firing. Temperature changes were not reported. The experiment consisted of a series of irradiations with a 40 mW laser over a 0.1 cm^2 area of forearm. The total energy applied at each irradiation was 1.2 J. The irradiance is, therefore, $I=400 \text{ mW}/\text{cm}^2$, which is within the range of power levels reported here. In a followup study by Lowe et al.,¹⁷ using the same paradigm, the latency in median nerve firing was shown to be consistent with small temperature changes during illumination. The authors point out that similar changes in nerve firing times can be obtained by any warming mechanism and is not specific to a direct photon interaction. They further observed temperature decreases of as much as 0.4°C below base line level postirradiation, which demonstrated a slow and cumulative response over the course of 20 min. The authors speculate that physiologic cooling mechanisms such as vasodilatation were brought into play. Similar effects are commonly observed after ultraviolet irradiation and are often as-

sociated with delay tissue damage. The mechanism for cooling is still speculative at best, though current work supports the idea that light causes a release of vasoactive substances in the upper dermal layers which then diffuse to the larger arterioles and trigger vasodilatation.^{16,31,32} However, it must be noted that for the near infrared study, while there was a strong correlation between temperature and latency there was no significant correlation between temperature change and absorbed energy in four out of five experimental protocols. During milder irradiation with a HeNe laser operating at 633 nm (0.95 mW for 20 s, $I = 19 \text{ mJ/cm}^2$). Basford et al.²⁹ and Greathouse, Currier, and Gilmore³⁰ measured no changes in nerve latency. In the later study temperature decreases were observed but were discounted due to instability in the ambient conditions. Finally, Danno and Sugie³³ used a rat model to show that exposure to near-infrared light ($I = 60 \text{ mW/cm}^2$, $\lambda = 970 \text{ nm}$) reversibly suppressed the ability of epidermal cells on the ear to proliferate and produced a 3°C temperature rise on the ear surface. This study was performed at a wavelength (970 nm) in which light absorption effects are significantly more pronounced in water than those used in optical topography (approximately 100× greater). Furthermore, the study employed halogen lamps, which illuminated the entire ear surface. We speculate that the larger temperature changes observed in this study are due to the large surface area of exposure and the large surface to volume ratio of the ear, which would not allow comparable conductive or radiative cooling. These reports demonstrate that interactions of light with biological systems are a complicated process which requires detailed evaluations for specific irradiation conditions, which consider irradiance (mW/cm^2), peak power (mW), total absorbed energy (J), and area irradiated (A) and system geometry.

5 Conclusions

Optical topography is a new method for visualizing cortical blood flow responses with high temporal resolution and high sensitivity to changes in chromophores such as hemoglobin and cytochrome. We have shown that during continuous illumination through a 1-mm-diam optical fiber, typical of current optical topography systems, the absorption induced heating is maximally estimated to be 0.11°C/mW, at a depth of 0.5 mm beneath the skin surface. Since our current optical topography systems run at a level of 1 mW, heating effects should be very small and well within safe limits. Finite element analysis shows that the small temperature changes are consistent with efficient thermal conduction from the irradiated region. Given the spatial distribution of temperature effects, fibers may be treated independently for inter-optode spacings greater than a few millimeters. These experiments imply that the irradiation did not elicit thermoregulatory responses. We recommend that similar measurements should be performed with pulsed laser systems to determine peak dermal temperatures and evaluate possible nonlinear effects, which are not present in CW systems. Such information will help to further our understanding of the complex interactions of light with biological systems.

Acknowledgments

The authors would like to thank Dr. A. Maki, Y. Yamashita, and Dr. T. Yamamoto of the Hitachi Central Research Laboratory for useful discussions and kind assistance throughout this project.

References

1. G. A. Milliken, "A simple photoelectric colorimeter," *J. Physiol. (London)* **79**, 152 (1933).
2. G. A. Milliken, "The oximeter, an instrument for measuring continuously the oxygen saturation of arterial blood in man," *Rev. Sci. Instrum.* **13**, 434–444 (1942).
3. F. F. Jobsis, "Noninvasive infrared monitoring of cerebral and myocardial oxygen sufficiency and circulatory parameters," *Science* **198**, 1264–1267 (1977).
4. J. C. Hebden and D. T. Delpy, "Diagnostic imaging with light," *Br. J. Radiol.* **70**, S206–S214 (1997).
5. M. Cope and D. T. Delpy, "System for long-term measurement of cerebral blood and tissue oxygenation on newborn infants by near infrared transillumination," *Med. Biol. Eng. Comput.* **26**, 289–294 (1988).
6. B. Chance, Z. Zhuang, C. Unah, C. Alter, and L. Lipton, "Cognition-activated low frequency modulation of light absorption in human brain," *Proc. Natl. Acad. Sci. USA* **90**, 3770–3774 (1993).
7. T. Kato, A. Kamei, S. Takashima, and T. Ozaki, "Human visual cortical function during photic stimulation monitoring by means of near infrared spectroscopy," *J. Cereb. Blood Flow Metab.* **13**, 516–520 (1993).
8. A. Villringer, J. Planck, C. Hock, L. Schleinkofer, and U. Dirnagl, "Near infrared spectroscopy (NIRS): A new tool to study hemodynamic changes during activation of brain function in human adults," *Neurosci. Lett.* **154**, 101–104 (1993).
9. Y. Hoshi and M. Tamura, "Detection of dynamic changes in cerebral oxygenation coupled to neuronal function during mental work in man," *Neurosci. Lett.* **150**, 5–8 (1993).
10. A. Maki, Y. Yamashita, Y. Ito, E. Watanabe, Y. Mayanagi, and H. Koizumi, "Spatial and temporal analysis of human motor activity using non-invasive NIR topography," *Med. Phys.* **22**, 1997–2005 (1995).
11. A. Maki, Y. Yamashita, E. Watanabe, and H. Koizumi, "Visualizing human motor activity by using non-invasive optical topography," *Front Med. Biol. Eng.* **7**(4), 285–297 (1996).
12. E. Watanabe, A. Maki, F. Kawaguchi, Y. Yamashita, H. Koizumi, and Y. Mayanagi, "Non-invasive assessment of language dominance with near-infrared spectroscopic mapping," *Neurosci. Lett.* **256**, 49–52 (1998).
13. E. Watanabe, A. Maki, F. Kawaguchi, Y. Yamashita, H. Koizumi, and Y. Mayanagi, "Non-invasive cerebral blood volume measurement during seizures using multichannel near infrared spectroscopic topography," *J. Epilepsy* **11**, 335–340 (1998).
14. W. C. Dewey, L. E. Hopwood, S. A. Sapareto, and L. E. Gerwick, "Cellular responses to combinations of hyperthermia and radiation," *Radiology* **123**(2), 463–474 (1977).
15. G. M. Hahn, *Hyperthermia and Cancer*, Plenum, New York (1982).
16. G. Kerfkens and J. C. van der Leun, "Skin temperature changes after irradiation with UVB or UVC: Implications for the mechanism underlying ultraviolet erythema," *Phys. Med. Biol.* **34**(5), 599–608 (1989).
17. A. S. Lowe, G. D. Baxter, D. M. Walsh, and J. M. Allen, "Effects of low intensity laser (830 nm) irradiation on skin temperature and antidromic conduction latencies in the human median nerve: Relevance of radiant exposure," *Lasers Surg. Med.* **14**, 40–46 (1994).
18. J. H. Sherman and D. S. Luciano, *Human Physiology: The Mechanisms of Body Function*, A. J. Vander, Ed., McGraw-Hill, New York (1994).
19. D. Sliney and M. Wolbarsht, *Safety With Lasers and Other Optical Sources: A Comprehensive Handbook*, Plenum, New York (1980).
20. G. M. Dusinberre, *Heat Transfer Calculations by Finite Differences*, International Textbook, Scranton, PA (1961).
21. *CRC Handbook of Chemistry and Physics*, 79th ed., D. R. Lide, Jr., Ed., CRC, Boca Raton, FL (1999).
22. "Near-infrared optical properties of ex vivo human skin and subcu-

- aneous tissues measured using the Monte Carlo inversion technique," *Phys. Med. Biol.* **43**, 2465–2478 (1993).
23. R. K. Hobbie, *Intermediate Physics for Medicine and Biology*, 3rd ed., Springer, New York (1997).
 24. W. C. Dewey and S. A. Sapareto, "Radiosensitization by hyperthermia occurs through an increase in chromosomal aberrations," Cancer therapy by hyperthermia and radiation, in *Proc. 2nd Int. Symp.*, Essen, Germany (June 1977).
 25. G. Pincus and A. Fischer, "The growth and death of tissue cultures exposed to supranormal temperatures," *J. Exp. Med.* **54**, 323–332 (1931).
 26. G. Huttmann and R. Biringruber, "Dynamics of thermal microeffects: Rate constants of thermal denaturation measured by a temperature-jump experiment," *Proc. Optical Society of America Trends in Optics and Photonics Biomedical Optical Spectroscopy and Diagnostics/Therapeutic Laser Applications*, Orlando, FL, pp. 300–305 (1998).
 27. R. Birngruber and V. Gabel, "Thermal verses photochemical damage in the retina-thermal calculations for exposure limits," *Trans. Ophthalmol. Soc. U.K.* **103**, 422–427 (1984).
 28. J. R. Basford, H. O. Hallman, J. Y. Matsumoto, S. K. Moyer, J. M. Buss, and G. D. Baxter, "Effects of 830 nm continuous wave laser diode irradiation on median nerve function in normal subjects," *Lasers Surg. Med.* **13**(6), 597–604 (1993).
 29. J. R. Basford, J. R. Daube, H. O. Hallman, T. L. Millard, and S. K. Moyer, "Does low intensity helium neon laser irradiation alter sensory nerve action or distal latencies?," *Lasers Surg. Med.* **10**, 25–39 (1990).
 30. D. G. Greathouse, D. P. Currier, and R. L. Gilmore, "Effects of clinical infrared laser on superficial radial nerve conduction," *Phys. Ther.* **65**, 1184–1187 (1985).
 31. N. R. Finsen, *Über die Bedeutung der chemischen Strahlen des Lichts für Medizin und Biologie*, Vogel, Leipzig (1899).
 32. T. H. Lewis, "The slower reactions of the skin to ultraviolet and to some other forms of stimulation, *The Blood Vessels of the Human Skin and Their Responses*, Shaw, London (1927).
 33. K. Danno and N. Sugie, "Effects of near-infrared radiation on the epidermal proliferation and cutaneous immune function in mice," *Photodermatol Photoimmunol Photomed* **12**, 233–236 (1996).